Highly Uniform Superparamagnetic Mesoporous Spheres with Submicrometer Scale and Their Uptake into Cells

Kyu Reon Lee,[†] Sol Kim,[‡] Dong Hyun Kang,[†] Jong In Lee,[†] Yoon Jie Lee,[†] Wan Seop Kim,[§] Deug-Hee Cho,[||] Heung Bin Lim,[⊥] Jungho Kim,[‡] and Nam Hwi Hur*[,†]

Department of Chemistry and Department of Life Science, Sogang University, Seoul 121-742, Korea, Physical Metrology Division, Korea Research Institute of Standards and Science, Daejeon 305-600, Korea, Advanced Chemical Technology Division, Korea Research Institute of Chemical Technology, Daejeon 305-600, Korea, and Department of Chemistry, Dankook University, Yongin, Gyeonggi-do 448-701, Korea

Received August 29, 2008. Revised Manuscript Received September 24, 2008

A new template approach was developed to synthesize highly uniform superparamagnetic mesoporous spheres with submicrometer scale, composed of silica and $CoFe_2O_4$, in which mesoporous shell/solid core silica spheres with an average diameter of 505 nm are used as templates. Superparamagnetic phases are grown exclusively within mesoporous shells of the host silica spheres using a mixed solvent composed of ethanol and dioctyl ether, which results in maintaining the mesoporous nature of the host silica and retaining the superparamagnetic property. The samples annealed at temperatures above 773 K are converted into high-crystalline forms with enhanced coercivity and magnetization, which show a type IV isotherm typical for the mesoporous silica. The resulting superparamagnetic spheres are well-dispersible in water, have high magnetization values, and possess high surface areas. Cellular viability studies showed that the particles were readily endocytosed in human breast cancer (MCF-7) and mouse embryonic fibroblast (NIH-3T3) cells. Such highly uniform superparamagnetic spheres with submicrometer scale are suitable for renewable supports for catalytic applications and magnetic carriers for drug delivery.

Introduction

Over the past decades, superparamagnetic nanoparticles (NPs) of spinel ferrites (MFe_2O_4; M = Fe, Co, Cu, Zn, etc) have drawn intense scientific and technological interests because they possess a wide range of applications in magnetic, catalytic, environmental, and biomedical fields.[1−8] Sustaining the superparamagnetic property of NPs is crucial for diverse applications mainly because it precludes magnetic aggregation and facilitates redispersion upon removal of a magnetic field. An inevitable drawback for the ferrite NPs is that their size should generally be less than about 30 nm in order to maintain their superparamagnetic property, which limits their usage particularly in biological affinity separations and drug delivery carriers.[9] An alternative way to overcome this size limit is that superparamagnetic particles with submicrometer scale were prepared by embedding superparamagnetic ferrites having average diameter of about 10 nm in a polymer matrix.[10−13] Similar inorganic congeners based on nontoxic silica have also been synthesized by assembling superparamagnetic NPs into a silica matrix in various ways.[14−19] However, the fabrication of these composites often encounters difficulties in achieving uniform loading of magnetic components and making the resulting NPs with highly uniform size, which is partly ascribed to the difficulty of dispersing the ferrite NPs evenly in a silica matrix in the course of the colloidal growth process.

Here we report the successful synthesis of highly uniform superparamagnetic mesoporous spheres (SMSs) with submicrometer scale, which provides the first demonstration of

* To whom correspondence should be addressed. Phone: 02 705 8440. Fax: 02 701 0967. E-mail: nhhur@sogang.ac.kr.
[†] Department of Chemistry, Sogang University.
[‡] Department of Life Science, Sogang University.
[§] Physical Metrology Division, Korea Research Institute of Standards and Science.
[||] Advanced Chemical Technology Division, Korea Research Institute of Standards and Science.
[⊥] Department of Chemistry, Dankook University.

(1) Fried, T.; Shemer, G.; Markovich, G. *Adv. Mater.* **2001**, *13*, 1158.
(2) Ye, X. R.; Daraio, C.; Wang, C.; Talbot, J. B.; Jin, S. *J. Nanosci. Nanotechnol.* **2006**, *6*, 852.
(3) Giri, S.; Trewyn, B. G.; Stellmaker, M. P.; Lin, V. S.-Y. *Angew. Chem., Int. Ed.* **2005**, *44*, 5038.
(4) Levy, L.; Sahoo, Y.; Kim, K.-S.; Bergey, E. J.; Prasad, P. N. *Chem. Mater.* **2002**, *14*, 3715.
(5) Elliott, D. W.; Zhang, W.-X. *Environ. Sci. Technol.* **2001**, *35*, 4922.
(6) Takafuji, M.; Ide, S.; Ihara, H.; Xu, Z. *Chem. Mater.* **2004**, *16*, 1977.
(7) Song, Q.; Zhang, Z. J. *J. Am. Chem. Soc.* **2004**, *126*, 6164.
(8) Yavuz, C. T.; Mayo, J. T.; Yu, W. W.; Prakash, A.; Falkner, J. C.; Yean, S.; Cong, L.; Shipley, H. J.; Kan, A.; Tomson, M.; Natelson, D.; Colvin, V. L *Science* **2006**, *314*, 964.
(9) Tong, X.-D.; Xue, B.; Sun, Y. *Biotechnol. Prog.* **2001**, *17*, 134.
(10) Ge, J.; Hu, Y.; Biasini, M.; Beyermann, W. P.; Yin, Y. *Angew. Chem., Int. Ed.* **2007**, *46*, 4342.
(11) Shang, H.; Chang, W.-S.; Kan, S.; Majetich, S. A.; Lee, G. U *Langmuir* **2006**, *22*, 2516.
(12) Xu, X.; Friedman, G.; Humfeld, K. D.; Majetich, S. A.; Asher, S. A. *Adv. Mater.* **2001**, *13*, 1681.
(13) Wang, Y.; Teng, X.; Wang, J.-S.; Yang, H. *Nano Lett.* **2003**, *3*, 789.
(14) Lu, Y.; Yin, Y.; Mayers, B. T.; Xia, Y. *Nano Lett.* **2002**, *2*, 183.
(15) Yoon, T.; Kim, J. S.; Kim, B. G.; Yu, K. N.; Cho, M.; Lee, J. *Angew. Chem., Int. Ed.* **2005**, *44*, 1068.
(16) Kim, J.; Lee, J. E.; Lee, J.; Jang, Y.; Kim, S.-W.; An, K.; Yu, J. H.; Hyeon, T. *Angew. Chem., Int. Ed.* **2006**, *45*, 4789.
(17) Hutlova, A.; Niznansky, D.; Rehspringer, J.-L.; Estournes, C.; Kurmoo, M. *Adv. Mater.* **2003**, *15*, 1622.
(18) Philipse, A. P.; van Bruggen, M. P.; B; Pathmamanoharan, C *Langmuir* **1994**, *10*, 92.
(19) Vestal, C. R.; Zhang, Z. J. *Nano Lett.* **2003**, *3*, 1739.

10.1021/cm802335r CCC: $40.75
Published on Web 10/22/2008

submicrometer-sized SMSs with easy control of size and magnetization. The SMSs composed of a silica core and a thin mesoporous magnetic shell were prepared using mesoporous shell/solid core silicas as template materials. The magnetic ($CoFe_2O_4$) phases are grown solely within mesopores of the shell while retaining the size of the host silica sphere. Despite their submicrometer size, they exhibit superparamagnetic behavior near 300 K because many nanocrystallites of $CoFe_2O_4$ reside only within the mesopores without agglomeration. In addition, the SMSs are well-dispersible in water because of their oxophilic surfaces, have high magnetization values when they are annealed, and possess high surface areas. More importantly, their size and magnetization can also be tuned simply by modifying the synthetic method and the annealing temperature, which makes them suitable for ideal renewable supports for catalytic and environmental applications.

Experimental Section

Synthesis of Mesoporous Shell/Solid Core Silica Spheres (*meso*-SiO_2). Silica spheres composed of mesoporous shell and solid core are prepared by slight modification of the Unger procedure.[20] In a 250 mL round-bottom flask, 75 mL of ethanol, 10 mL of deionized water, and 3 mL of ammonia were mixed, which was stirred for 10 min. To the solution, 6 mL of TEOS (tetraethoxysilane, 98%, Aldrich) was added and vigorously stirred. After stirring for 2 h, a mixture of 5 mL of TEOS and 2 mL of C18TMS (n-octadecyltrimethoxysilane, 85%, TCI) was added under vigorous stirring for 2 h. The resulting mesoporous shell/solid core silica spheres (meso-SiO_2) beads were collected by centrifugation, which were then dried in air to yield a white powder. To remove all organic residues incorporated in the silica, we sintered the powder in air at 823 K for 6 h.

Synthesis of Superparamagnetic Mesoporous Spheres $CoFe_2O_4$@SiO_2. For the synthesis of superparamagnetic colloidal spheres, 1 g of *meso*-SiO_2 was added into a 10 mL of ethanol with vigorous stirring and sonicating to disperse the silica beads completely. To the solution were added 0.0975 g of $Co(NO_3)_2 \cdot 6H_2O$ (98+%, Aldrich) and 0.2705 g of $Fe(NO_3)_3 \cdot 9H_2O$ (98+%, Aldrich). After complete dissolution of the Co and Fe precursors, 30 mL of dioctyl ether (99%, Aldrich) and 1 mL of Igepal CO-520 (Aldrich) were added into the mixed solution, followed by stirring and sonicating for 10 min. The reaction mixture was heated to 363 K with stirring until ethanol was almost completely evaporated. The mixture was then further refluxed at 573 K for 6 h. The resultant colloidal silica beads with dark brown color were separated by centrifugation (1500 rpm) with a couple of intermediate disperses in ethanol. By using a magnet, finally, the product denoted as $CoFe_2O_4$@SiO_2 was collected and washed with ethanol several times, which was dried in an oven set at 353 K. The as-prepared SMSs were annealed at 573, 773, and 973 K in air for 24 h. the resulting three samples were completely characterized by various means. They are virtually identical in shape but have slightly different magnetic and surface properties.

Loading of Rhodamine to $CoFe_2O_4$@SiO_2 Superparamagnetic Mesoporous Spheres. To a 10 mL solution of CH_3CN were added $CoFe_2O_4$@SiO_2 SMSs (0.5 g), and Rhodamine101 dye (5 mg), and the solution was sonicated. The reaction mixture was stirred at 333 K for 12 h. The resultant dye-loaded SMSs were collected by a magnet and washed with ethanol several times.

Cell Localization. Human breast cancer (MCF-7) or mouse embryonic fibroblast (NIH-3T3) cells were plated at a density of 8×10^4 per 60 mm dish and cultured in Dulbecco's modified Eagle's medium (DMEM) supplemented with 10% heat-inactivated fetal calf serum (Hyclone), penicillin, and streptomycin for 24 h at 310 K. Fresh Rhodamine- conjugated SMSs were then added to NIH3T3 or MCF-7 cells (final conc. 100 μg/mL) and incubated for 24 h. For fluorescence detection, treated and controlled cells were washed in PBS, fixed for 10 min at 253 K with an acetone/methanol mixture (1:1, v/v), and then briefly washed and rehydrated in PBS (277 K). To examine the localization of Rhodamine conjugated superparamagnetic spheres, we measuered fluorescence signals using a fluorescence microscope (Olypus, IX71) equipped with DP71.

Characterizations and Measurements. Powder X-ray diffraction patterns were recorded with a Rigaku DMAX 2500 diffractometer (Cu Kα) operating at 40 kV and 150 mA. TEM analyses were carried out using a JEOL JEM-2100F. Samples for TEM were prepared by dropping the diluted sample in ethanol on a 400 mesh carbon-coated copper grid. The temperature-dependent and field-dependent magnetization measurements were measured with a Quantum Design MPMS-5 SQUID magnetometer. The temperature dependence of the magnetic susceptibility was investigated on a powder sample from 5 to 350 K in an applied magnetic field of 100 G. DC magnetization measurements were made after cooling the sample both in zero-field-cooled (ZFC) and field-cooled (FC) magnetic conditions. The field-dependent magnetization was measured at 10 and 300 K.

Nitrogen Sorption Measurements. Adsorption and desorption measurements were performed using an ASAP 2420 instrument (Micrometrics) with nitrogen as adsorptive at 77.3 K. The BET surface areas were calculated from $p/p_0 = 0.05-0.3$ in the adsorption curve using a BET equation. The pore size distributions were calculated from the desorption curve using the DFT method. Prior to each sorption measurement, the sample was outgassed at 300 °C for 24 h under vacuum to remove all the impurities completely.

Quantitative Analysis of Fe and Co Contents in $CoFe_2O_4$@SiO_2 by ICP-MS. About 0.005 g of $CoFe_2O_4$@SiO_2 was weighed and transferred into a vessel for microwave acid digestion. Then, 2 mL of HF, 2 mL of H_2SO_4, and 5 mL of HNO_3 were added into the vessel, followed by the programmed procedure for the digestion. The digested sample solutions were cooled to room temperature, which were delivered into a 100 mL volumetric flask. After the solutions were properly diluted, the Fe and Co contents in the solution were determined by ICP-MS. Weight percentages of Co and Fe are 1.428 and 2.427%, respectively.

Results and Discussion

A schematic diagram of the synthetic procedure is illustrated in Figure 1. Highly unform silica spheres composed of mesoporous shell and solid core are used as parent materials, which are prepared by slight modification of the Unger procedure.[20] The silica spheres with uniform diameter are synthesized on the basis of the well-established colloidal chemistry combined with the sol−gel process. The key step of our approach is to load magnetic components exclusively into mesoporous shell of the host silica, which leads to the growth of cobalt ferrite phases within the pores rather than the outside shell. This eventually results in sustaining superparamagnetic property and retaining the spherical shape of the host silica. The synthesis is accomplished by using a mixed solvent in which an ethanol solution containing cobalt and iron precursors is dispersed into a dioctyl ether matrix.

(20) Büchel, G.; Unger, K. K; Matsumoto, A.; Tsutsumi, K. *Adv. Mater.* **1998**, *10*, 1036.

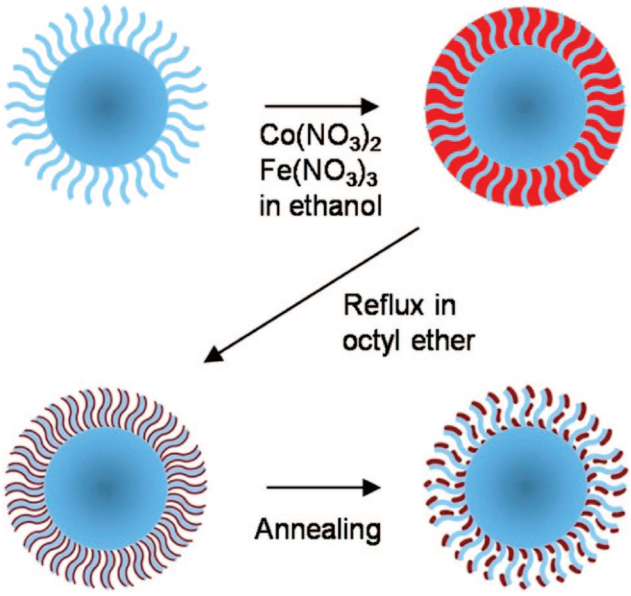

Figure 1. Schematic diagram of the pathway to the synthesis of a $CoFe_2O_4$@SiO_2 SMS using a mesoporous shell/solid core silica. Red dots inside the shell represent the $CoFe_2O_4$ phase.

The two liquid phases immiscible in the initial stage are gradually homogenized to yield one nonaqueous phase, which is accomplished by slow evaporation of ethanol. Subsequent refluxing at 573 K leads to the infiltration of the Co and Fe precursors into the porous shell. With increasing the temperature, cobalt ferrite phases are grown inside the pores without changing the host silica framework. Finally, the resulting products, $CoFe_2O_4$@SiO_2 SMSs, are rinsed with ethanol several times to remove organic residues.

The X-ray diffraction (XRD) patterns for the $CoFe_2O_4$@-SiO_2 SMSs annealed at 573, 773, and 973 K in air are shown in Figure 2. Although the XRD peaks of the sample at 573 K are very broad, they can well index to the patterns expected

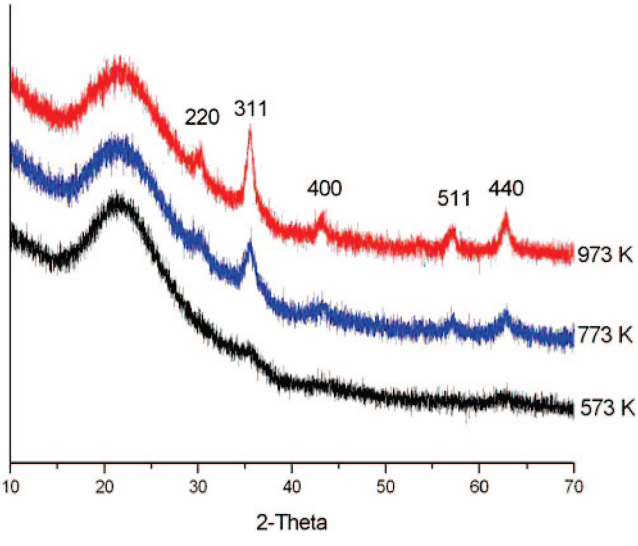

Figure 2. Powder XRD patterns for the $CoFe_2O_4$@SiO_2 SMSs annealed at 573, 773, and 973 K. Vertical bars below the XRD patterns represent the theoretical peak positions of $CoFe_2O_4$. A very broad peak about $2\theta = 22°$ is due to SiO_2.

for the cubic spinel phase (space group: *Fd*3*m*).[21] The broad feature of the peaks indicates the presence of the nanometer-sized grains. The average grain size calculated by using a Debye−Scherrer equation is 8.6 nm.[22] Annealing the same SMSs at 773 and 973 K still retains the same XRD patterns but their XRD peaks become noticeably narrow, indicating an increase in the grain size. In fact, average particle sizes of the samples annealed at 773 and 973 K, estimated from the same equation, are 11.3 and 15.3 nm, respectively, suggesting that nanocrystallites are evolved within the mesoporous silica shell only. Namely, gradual growth of nanocrystallites of cobalt ferrite by high-temperature annealing is limited by the confinement effect of the mesopores in the shell.

Transmission electron microscope (TEM) images of the three samples are illustrated in Figure 3, showing that all the SMSs have almost perfectly spherical shape with a core/shell structure and the pores are randomly distributed in the shell. Regardless of post heating temperatures, in addition, sizes of all the $CoFe_2O_4$@SiO_2 SMSs are virtually identical where average diameters of core and shell are 410 and 95 nm, respectively. The 973 K sample exhibits slightly darker TEM image than the 573 K one, which is due mainly to better crystalline order of the 973 K sample. Moreover, the SMSs sintered at 973 K do not show any indication of agglomeration. The TEM data indicate that the $CoFe_2O_4$ phases are completely embedded within the mesoporous shell of about 95 nm thicknesses, which is consistent with the XRD data. Selected area electron diffraction patterns are also consistent with the XRD data and confirm a single-phase cubic spinel structure for the three SMSs (see the Supporting Information).

This conjecture associated with the growth mechanism of the $CoFe_2O_4$ phase is also evidenced by the surface characteristics studied by the Brunauer−Emmett−Teller (BET) method. In Figure 4, the nitrogen sorption isotherms and the pore size distributions of the three $CoFe_2O_4$@SiO_2 SMSs annealed at 573, 773, and 973 K are displayed along with those of the parent mesoporous SiO_2. The 573 K sample shows like a type II isotherm, indicating that its pores might have microporous characteristics.[23,24] However, the two samples at 773 and 973 K show a type IV isotherm, which is typical for mesoporous silica. The results suggest that at the initial stage of the growth process the parent meso-SiO_2 with a type IV isotherm is transformed to a type II-like isotherm by the filling of mesopores in the shell with the $CoFe_2O_4$ precursor. Upon annealing the sample at temperature above 773 K, organic residues are completely removed and the loosely bound $CoFe_2O_4$ crystallites are tightly stuck on the silica surface. The high temperature annealing leads to the formation of dense samples with high crystalline order, which results in increments of pore volume and pore size of

(21) Zhao, L; Zhang, H.; Zhou, L.; Xing, Y.; Song, S.; Lei, Y. *Chem. Commun.* **2008**, 3570.
(22) West, A. R. *Solid State Chemistry and Its Applications*; Wiley: New York, 1984.
(23) Brunauer, S.; Deming, L. S.; Deming, W. E.; Teller, E. *J. Am. Chem. Soc.* **1940**, *62*, 1723.
(24) Ravikovich, P. I.; Neimark, A. V. *Colloids Surf., A* **2001**, *187*−*188*, 11.

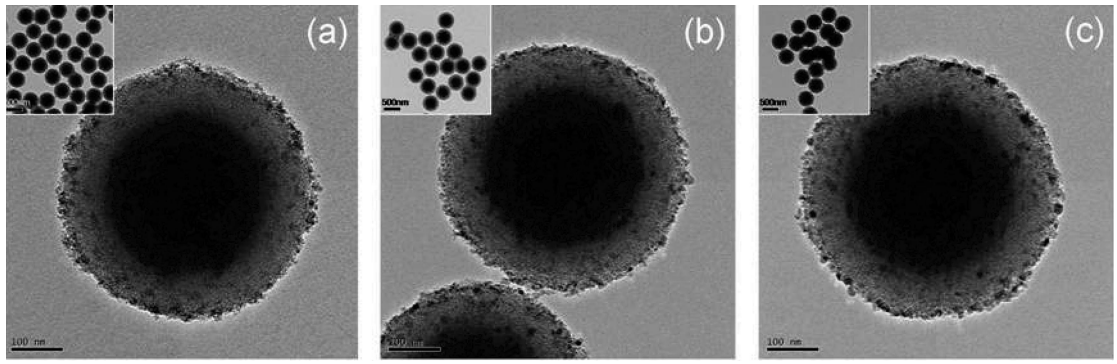

Figure 3. Typical TEM micrographs of the $CoFe_2O_4$@SiO_2 SMSs annealed at (a) 573, (b) 773, and (c) 973 K, showing that all the SMSs have virtually identical shapes regardless of the annealing temperature. Left insets are expanded TEM images of corresponding SMSs.

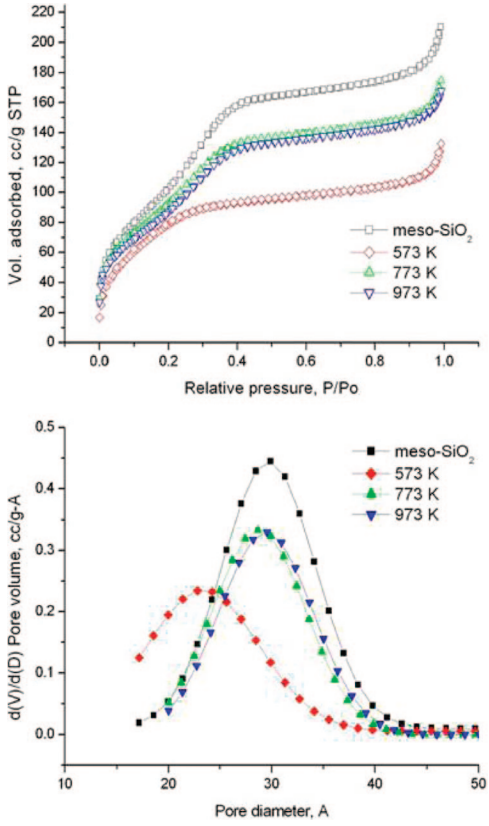

Figure 4. Nitrogen adsorption/desorption isotherms and pore size distributions of the three $CoFe_2O_4$@SiO_2 SMSs annealed at 573, 773, and 973 K. For comparison, the isotherm and pore size distribution of the parent *meso*-SiO_2 were included.

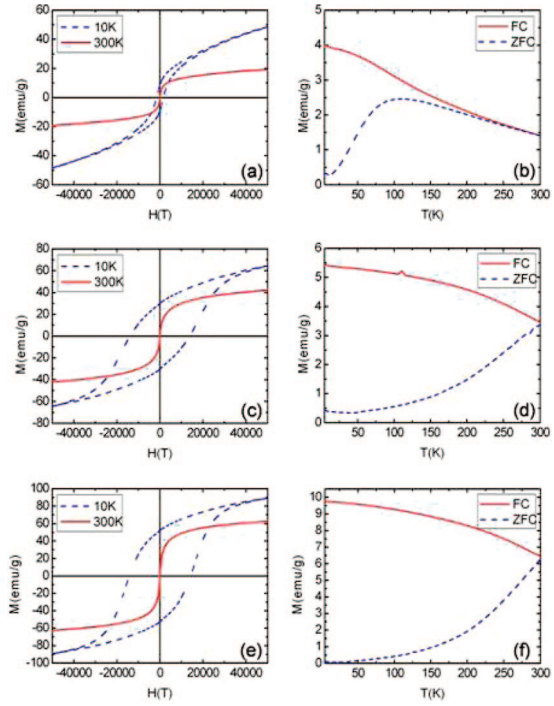

Figure 5. Field-dependent magnetization curves of the $CoFe_2O_4$@SiO_2 SMSs annealed at (a) 573, (c) 773, and (e) 973 K, measured at 10 and 300 K. Temperature-dependent magnetization curves of the same SMSs at (b) 573, (d) 773, and (f) 973 K, which were measured at 100 G. Open and filled symbols represent field-cooled and zero-field-cooled magnetization data, respectively.

the SMSs annealed at 773 and 973 K by comparison with those of the 573 K sample. Accordingly, the two SMSs show the type IV isotherms, which are quite analogous to that of the parent meso-SiO_2. Values of BET surface area, total pore volume, and pore diameter of the $CoFe_2O_4$@SiO_2 SMSs are listed in Table S1 of the Supporting Information. It is worthwhile to mention that the $CoFe_2O_4$@SiO_2 SMSs have randomly distributed mesopores as found in the parent silica template.

To assess their magnetic response to an external field, we collected the field- and temperature-dependent magnetization data of the $CoFe_2O_4$@SiO_2 SMSs using a SQUID magnetometer. The magnetic hysteresis curves of the 573 K sample, given in Figure 5, display almost neither coercivity nor saturation even at high magnetic field, which are indicative of superparamagnetic characters. Their coercivity at 10 K, however, is sensitive to the annealing temperature. Upon increasing the heating temperature, the coercivity of the annealed sample increased, suggesting the progressive growth of magnetic ferrite phases by high temperature annealing. This size dependence of coercivity indicates that the $CoFe_2O_4$ phases exist as single domains. As the particle size increases below a critical diameter, the coercivity increases because of thermal effect.[25] The magnetization values also increased with increasing the annealing temperature but their magnitudes are still lower relative to bulk $CoFe_2O_4$ form, which is ascribed to the presence of superparamagnetic phases in the $CoFe_2O_4$ phases.

A magnetization versus temperature curve for the 573 K sample, shown in Figure 5, also confirms its superparamagnetism. Its blocking temperature (T_B), where thermal fluctuations randomize the aligned spins, is about 100 K. For the

samples annealed at 773 and 973 K, their blocking temperatures are close to the bifurcation temperatures between the field-cooled and zero-field-cooled curves mainly because magnetic domain sizes are increased. Clearly, the three samples show superparamagnetic behavior, while they retain the inherent characteristics of mesoporous shell silica including high surface area and micrometer-scale particle size. One thing to be addressed is that magnitudes of magnetization and coercivity of the $CoFe_2O_4@SiO_2$ SMSs can be tuned by the post annealing temperature.

To check the possibility of the $CoFe_2O_4@SiO_2$ SMSs as drug carriers, cellular uptakes of the SMSs were examined by taking fluorescence microscope images of both immortalized mouse fibroblast (NIH-3T3) and human breast cancer (MCF-7) cells with the dye-loaded SMSs. For this study Rhodamine 101 was used as a fluorescent dye, which was tightly bound to the ferrite surface through the bonding between the carboxylate groups on the dye molecule and the hydroxyl groups on the oxide surface. As can be seen in fluorescent micrographs of NIH-3T3 and MCF-7 cells treated with the dye-loaded SMSs (Figure 6), the SMSs were apparently endocytosed and were internalized by the cells rather than bound to their surfaces. A deeper look at the micrographs reveals that most of the SMSs appeared as red dots are located in the lysosomes of the cells, suggesting that the SMSs can serve as therapeutic drug carriers. In addition, they can potentially serve as contrast agents in MRI because of their superparamagnetic properties.[26−29]

Conclusion

Using mesoporous shell/solid core silica templates, we have developed a novel method for synthesizing SMSs with submicron size that have high porosities and large surface areas. Although we have demonstrated a couple of cellular uptakes using the SMSs in the present experimental work, the unprecedented porous SMSs could be applicable to a wide range of renewable supporting materials for catalytic and environmental applications. This new technique shows promise for being a general approach to the synthesis of a wide range of new porous micrometer-sized materials with interesting properties simply by infiltrating various precursors into the same mesoporous silica shells, which is currently underway.

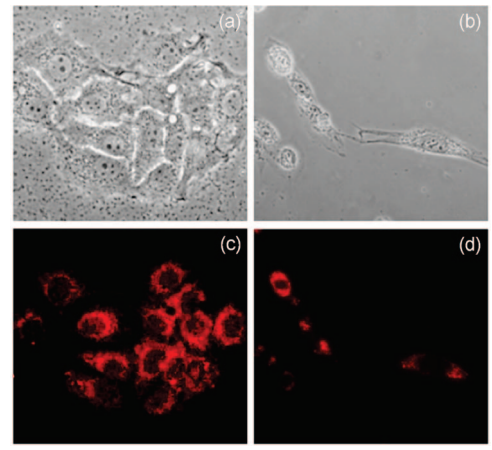

Figure 6. Optical microscope images (×400) of (a) MCF-7 and (b) NIH-3T3 cells treated with dye-loaded $CoFe_2O_4@SiO_2$ SMSs. Corresponding fluorescent microscope images (×400) of (c) MCF-7 and (d) NIH-3T3.

Acknowledgment. This work was supported by the KOSEF grant funded by MOST in Korea (ROA-2007-000-20088-0). Acknowledgement also goes to the BK 21 Programs and the Interdisciplinary Program of Integrated Biotechnology at Sogang University.

Supporting Information Available: Selected area electron diffraction patterns, BET surface data, ICP-MS analyses, and fluorescence microscopy images (PDF). This material is available free of charge via the Internet at http://pubs.acs.org.

CM802335R

(25) Cullity, B. D. *Introduction to Magnetic Materials*; Addison-Wesley: Reading. MA, 1972.
(26) Ow, H.; Larson, D. R.; Srivastava, M.; Baird, B. A.; Webb, W. W.; Wiesner, U. *Nano Lett.* **2005**, *5*, 113.
(27) Lauffer, R. B. *Chem. Rev.* **1987**, *87*, 901.
(28) Martina, M. S.; Fortin, J. P.; Menager, C.; Clement, O.; Barratt, G.; Grabielle-Madelmont, C.; Gazeau, F.; Cabuil, V.; Lesieur, S. *J. Am. Chem. Soc.* **2005**, *127*, 10676.
(29) Huh, Y.-M.; Jun, Y.-W.; Song, H.-T.; Kim, S.; Choi, J.-S.; Lee, J.-H.; Yoon, S.; Kim, K.-S.; Shin, J.-S.; Suh, J.-S.; Cheon, J. *J. Am. Chem. Soc.* **2005**, *127*, 12387.